^{13}C NMR Study of Effects of Fasting and Diabetes on the Metabolism of Pyruvate in the Tricarboxylic Acid Cycle and of the Utilization of Pyruvate and Ethanol in Lipogenesis in Perfused Rat Liver

Sheila M. Cohen

Department of Biophysics, Merck Institute for Therapeutic Research, Merck Sharp & Dohme Research Laboratories, Rahway, New Jersey 07065

Received March 17, 1986; Revised Manuscript Received September 25, 1986

ABSTRACT: ^{13}C NMR has been used to study the competition of pyruvate dehydrogenase with pyruvate carboxylase for entry of pyruvate into the tricarboxylic acid (TCA) cycle in perfused liver from streptozotocin-diabetic and normal donor rats. The relative proportion of pyruvate entering the TCA cycle by these two routes was estimated from the ^{13}C enrichments at the individual carbons of glutamate when [3-^{13}C]alanine was the only exogenous substrate present. In this way, the proportion of pyruvate entering by the pyruvate dehydrogenase route relative to the pyruvate carboxylase route was determined to be 1:1.2 ± 0.1 in liver from fed controls, 1:7.7 ± 2 in liver from 24-fasted controls, and 1:2.6 ± 0.3 in diabetic liver. Pursuant to this observation that conversion of pyruvate to acetyl coenzyme A (acetyl-CoA) was greatest in perfused liver from fed controls, the incorporation of ^{13}C label into fatty acids was monitored in this liver preparation. Livers were perfused under steady-state conditions with labeled substrates that are converted to either [2-^{13}C]acetyl-CoA or [1-^{13}C]acetyl-CoA, which in the de novo synthesis pathway label alternate carbons in fatty acids. With the exception of the repeating methylene carbons, fatty acyl carbons labeled by [1-^{13}C]acetyl-CoA (from [2-^{13}C]pyruvate) gave rise to resonances distinguishable on the basis of chemical shift from those observed when label was introduced by [3-^{13}C]alanine plus [2-^{13}C]ethanol, which are converted to [2-^{13}C]acetyl-CoA. Thus, measurement of ^{13}C enrichment at several specific sites in the fatty acyl chains in time-resolved spectra of perfused liver offers a novel way of monitoring the kinetics of the biosynthesis of fatty acids. In addition to obtaining the rate of lipogenesis, it was possible to distinguish the contributions of chain elongation from those of the de novo synthesis pathway and to estimate the average chain length of the ^{13}C-labeled fatty acids produced. Finally, the proportion of the product of the de novo synthesis pathway that served as precursor for monoenoic acid was estimated from the time course for ^{13}C enrichment at the olefinic fatty acyl carbon.

Carbon-13 NMR spectroscopy provides a useful approach to the study of metabolism in cells, isolated perfused organs, and whole animals (Cohen et al., 1981; Cohen, 1983; Cross et al., 1984; Neurohr et al., 1984; Reo et al., 1984). When substrates specifically labeled with ^{13}C are administered, signals are measured, repetitively, from substrate, intermediates, and end products. Because the operation and regulation of the enzymes of intermediary metabolism must ultimately be understood within the context of the physiology of the whole cell, it is useful to exploit the nondestructive ^{13}C NMR method and its special properties to complement more familiar approaches, such as in vitro studies with purified enzymes and ^{14}C tracer investigations of metabolism.

Pyruvate is an important branch point (Krebs, 1957) both in the catabolic sequence of glucose and in the gluconeogenic pathway from substrates, such as alanine, that enter the pathway below the level of the triose phosphates. In rat liver, pyruvate can enter the tricarboxylic acid (TCA) route in two different ways: by carboxylation to form a dicarboxylic acid through the activity of pyruvate carboxylase or by oxidative decarboxylation to acetyl-CoA via the activity of pyruvate dehydrogenase. The other major pathway of pyruvate metabolism in liver is catalyzed by pyruvate kinase. As described in the preceding paper, flux through pyruvate kinase in perfused liver from streptozotocin-diabetic rats and their untreated littermates has been determined by a ^{13}C NMR assay, and the acute regulation of this enzyme by insulin has been demonstrated (Cohen, 1987b). In a previous study (Cohen, 1987a), ^{13}C NMR was used to investigate the gluconeogenic pathway from alanine or pyruvate and to identify metabolites in perfused liver from the streptozotocin-treated rat model of type 1 diabetes and from normal control rats. While flux through pyruvate dehydrogenase in these preparations was touched upon in the two previous papers, this investigation expands upon this aspect and focuses on a ^{13}C NMR determination of the flux into the TCA cycle through pyruvate dehydrogenase relative to that through pyruvate carboxylase in perfused liver from diabetic rats and from fed and fasted normal rats. The relative proportion of pyruvate entering the TCA cycle by these two routes is estimated from the ^{13}C enrichments at the individual carbons of glutamate in perfused liver when [3-^{13}C]alanine is the only exogenous substrate present. The liver preparations examined provided large gradations in relative flux through pyruvate dehydrogenase and demonstrate the utility of the ^{13}C NMR approach in evaluating factors responsible for directing the pathway chosen.

Of the liver preparations examined here, the proportion of pyruvate entering the TCA cycle as acetyl-CoA was determined to be greatest in liver from fed control donor rats. This observation is consistent with the well-recognized maximal contribution of acetyl-CoA to the cytosolic process of fatty acid synthesis in liver of fed normal rats (Van Golde & Van den Bergh, 1977), Consequently, it seemed worthwhile to draw upon the inherent capacity of ^{13}C NMR for the simultaneous

0006-2960/87/0426-0581$01.50/0 © 1987 American Chemical Society

observation in a single spectrum of resonances of individual carbon atoms in all metabolites labeled to the level of detection (ca. 0.2 mM in ^{13}C) and to follow the incorporation of ^{13}C label in fatty acids in perfused liver from fed normal rats. In livers perfused under steady-state conditions with [3-^{13}C]alanine and [2-^{13}C]ethanol, both of which are converted to [2-^{13}C]-acetyl-CoA, it was possible to follow in real time ^{13}C enrichment at several discrete sites in fatty acyl chains that are appropriate for incorporation of [2-^{13}C]acetyl-CoA via the de novo synthesis pathway. The delayed appearance of a resonance representing olefinic carbon in monoenoic fatty acids is consistent with the operation of an additional, desaturation step. To demonstrate the specificity of this approach, other livers from fed rats were perfused with [2-^{13}C]pyruvate, which is converted to [1-^{13}C]acetyl-CoA in the TCA cycle. ^{13}C spectra of these livers followed the ^{13}C enrichment at specific positions in the fatty acyl chains appropriate for incorporation of [1-^{13}C]acetyl-CoA by the de novo synthesis pathway. With the exception of the repeating methylene carbon, fatty acyl carbons labeled by [1-^{13}C]acetyl-CoA gave rise to resonances that could be distinguished on the basis of chemical shift from those observed when label was introduced by substrates that were converted to [2-^{13}C]acetyl-CoA. Thus, by following the ^{13}C enrichment at several specific positions in the fatty acyl chains in the time-sequential spectra of perfused liver from fed normal rats, the kinetics of the biosynthesis of fatty acids can be monitored in a novel way by ^{13}C NMR.

Materials and Methods

All experimental conditions were as given previously (Cohen, 1987a), including the preparation of the animals, NMR conditions, and method of liver perfusion. As described before in detail, for each perfused liver the data collected included ^{31}P NMR spectra at 145.8 MHz of the perfused liver before and after measurement of the ^{13}C NMR data, ^{13}C NMR spectra at 90.5 MHz of the perfused liver before and after the addition of substrate, and ^{13}C NMR spectra of the perchloric acid extract prepared from the freeze-clamped liver. As usual, each liver went through a lengthy (30–40-min) preliminary period during which substrate-free perfusate was not recirculated so as to deplete and wash out endogenous substrates.

To provide adequate time resolution, NMR acquisition parameters were chosen to maximize signal-to-noise by using pulse repetition rates that were usually less than $5T_1$; because this procedure results in some resonances being partially saturated, peak intensities in the ^{13}C NMR spectra were corrected for T_1 effects. All spectral intensities used in calculations here were corrected for nuclear Overhauser effect (NOE) and T_1 effects as described in detail before (Cohen, 1987a); the correction procedures used were tailored for the particular calculation involved and are similar to those used previously in ^{13}C NMR studies of perfused rat liver (Cohen, 1983) and of red blood cells (Oxley et al., 1984). Calibration the peak intensities of labeled fatty acids synthesized by rat liver required a modified approach that used (1) previous measurements of T_1 and NOE for the individual carbon atoms in the fatty acyl chains of triacylglycerols at the natural abundance of ^{13}C in perfused rat liver (Canioni et al., 1983) and (2) peak intensities of endogenous fatty acids in the copious triacylglycerols present in liver from genetically obese mice measured in ^{13}C NMR spectra acquired under our exact conditions. Liver from the ob/ob mouse was considered to be a more representative reference model for this purpose than a solution of a triacylglycerol. The donor mouse was a male (C57BL/6J ob/ob), 16 weeks of age (Jackson Laboratories, Bar Harbor, ME), fasted 24 h; our standard perfusion conditions were used for the ob/ob liver.

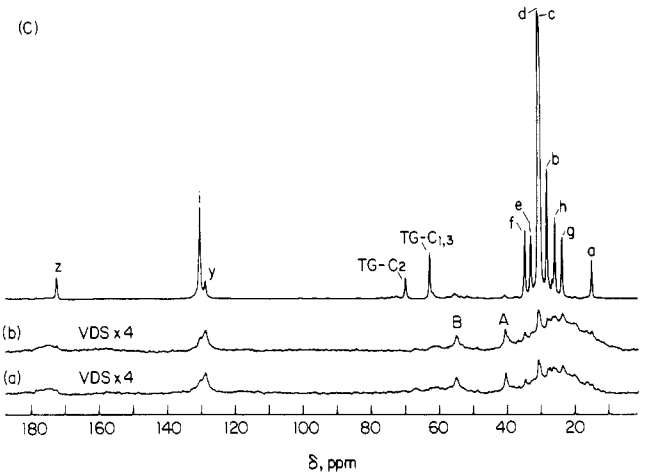

FIGURE 1: ^{13}C NMR spectra at 90.5 MHz showing ^{13}C natural abundance background of isolated perfused livers at 35 ± 1 °C before the addition of labeled substrate. Livers were from (a) 24-h-fasted normal control rat, (b) fed normal control rat, and (c) 24-h-fasted ob/ob mouse. Labeled resonances are identified in Table I. The notation VDS × 4 indicates that the gain on the vertical axis was increased 4-fold when spectra a and b were read out as compared with spectrum c.

Results

The natural abundance of ^{13}C is only 1.1%. Consequently, only metabolites with high intracellular concentrations are detectable at the natural abundance level by ^{13}C NMR. In liver these metabolites are typically storage compounds such as glycogen (Stevens et al., 1982) or triacylglycerols (Cohen et al., 1979; Block, 1982; Canioni et al, 1983). The ^{13}C natural abundance background of perfused liver from a 24-h-fasted normal rat and a fed normal rat are shown in spectra a and b of Figure 1, respectively. Background spectra of liver from streptozotocin-diabetic rats resemble Figure 1a very closely and are therefore not shown. As an aid in the assignment of the resonances arising from the natural abundance background of triacylglycerols in rat liver, spectra a and b of Figure 1 are contrasted with the ^{13}C natural abundance background spectrum of a perfused liver from a genetically obese ob/ob mouse (Figure 1c). The triacylglycerol content of ob/ob liver is extremely high, reaching about 250 μmol/g of liver wet weight in liver from the 16-week-old mouse, as is shown here (Menahan, 1983). The assignments of the labeled resonances in Figure 1 are listed in Table I. The resonances attributable to carbon atoms in fatty acyl chains in triacylglycerols in the ob/ob liver shown in Figure 1c have an average full width at half-height of only 41 ± 6 Hz, with 20-Hz line broadening applied. As was noted in an earlier ^{13}C NMR study of perfused mouse liver (Cohen et al., 1979), triacylglycerols are present in liver as neutral fat droplets and therefore give rise to relatively sharp NMR peaks. The ^{13}C NMR resonances of endogenous triacylglycerols in liver from normal or diabetic rats were in all cases under our conditions of much lower relative intensity than those measured in liver from even normal mouse, presumably reflecting species differences in relative triacylglycerol content. The ^{13}C natural abundance spectrum of ob/ob liver (Fig. 1c), on the other hand, is similar to that of adipose tissue (Williams et al., 1973; Canioni et al., 1983). The absence of resonances of glycogen in the background spectrum of liver from the fed rat (Figure 1b) is attributed to its depletion during an initial 40-min period of substrate-free perfusion during which the perfusion fluid was not recirculated.

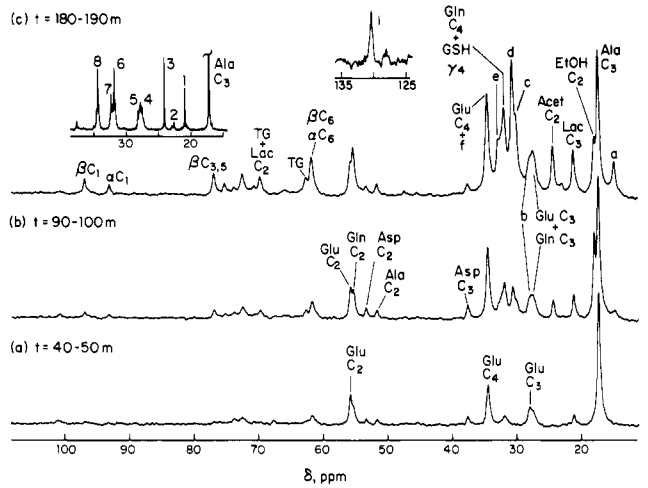

FIGURE 2: ^{13}C NMR spectra of perfused liver from a fed normal rat at 35 ± 1 °C. (a) Spectrum 40–50 min after the addition of 10.0 mM [3-^{13}C]alanine. Spectrum b was accumulated during the interval 90–100 min after the addition of [3-^{13}C]alanine and 40–50 min after addition of 7.3 mM [2-^{13}C]ethanol. (c) Spectrum measured 180–190 min after the initial addition of [3-^{13}C]alanine and 130–140 min after initial addition of [2-^{13}C]ethanol. Substrate was maintained at or near these levels. Each spectrum represents 800 scans acquired as described in text. The ^{13}C natural abundance background spectrum of this liver was accumulated under identical conditions before the addition of substrate; this background spectrum was subtracted from each spectrum measured postsubstrate. The right-hand insert shows the 125–135 ppm region of spectrum c; the vertical gain was increased 7-fold when the 125–135 ppm region was read out. The labeled ^{13}C NMR peaks include those due to the α and β anomers of D-glucose: βC-1, αC-1, to βB-6, αC-6; Glu, glutamate; Gln, glutamine; Asp, aspartate; GSH γ4, glutathione γ-glutamyl C-4; Ala, alanine; Acet, acetate; Lac, Lactate; EtOH, ethanol. Peaks a–f, i, and TG are assigned in Table I. The left-hand insert shows the ^{13}C NMR spectrum of the perchloric acid extract of this liver, which was freeze-clamped shortly after spectrum c was recorded. The pH of the extract was 7.80. The region from 15 to 40 ppm is shown; this spectrum required 9600 pulses of 30° free-induction decays, with 2.3-s recovery time between pulses. The NMR sample temperature was 12 °C for this extract. The numbered peaks in this insert include the following: 1, lactate C-3; 2, β-hydroxybutyrate C-4; 3, acetate C-2; 4, glutamine C-3 and GSHγ-3; 5, glutamate C-3; 6, glutamine C-4; 7, GSHγ-4; 8, glutamate C-4.

Thus, the ^{13}C natural abundance resonances of perfused rat liver under our conditions are of relatively low intensity. The ^{13}C natural abundance background spectrum of each given liver is subtracted from each spectrum accumulated after the addition of ^{13}C-labeled substrate for ease of interpretation. This procedure was followed for each of the spectra shown in Figure 2. Elimination of the background resonance at 40.4 ppm, labeled A in Figure 1, is a good test of the cleanness of the subtraction procedure because no signals from ^{13}C-labeled metabolites interfer with peak A. Indeed, the closest possible resonance, that arising from *N*-carbamoylaspartate C-3, resonates almost 1 ppm downfield from peak A and is thus clearly resolved. Inspection of the 40.4 ppm region in the three spectra shown in Figure 2, as well as the spectra shown in the two related papers, indicates that the subtraction was clean and essentially complete under these conditions. Subtraction of the background peaks at 130.3 and 128.7 ppm, labeled i and y, respectively, in Figure 1, and the broad region at 175 ppm was also demonstrated to be clean and essentially complete under our conditions (not shown). The validity of the subtraction procedure used to eliminate the ^{13}C natural abundance background of each liver is emphasized because the ^{13}C enrichments measured in metabolites in spectra accumulated after the addition of labeled substrate are used here to estimate in situ fluxes in liver.

Table I: Chemical Shifts and Assignments of Lipid Resonances Observable at the Natural Abundance of ^{13}C in Perfused Liver from ob/ob Mouse[a]

resonance	assignment	chemical shift (ppm)
a	*CH_3CH_2–	14.73
b	—CH_2*CH_2CH=CH—	27.95
c	fatty acyl –(*CH_2)–	30.18
d		30.51
e	CH_3CH_2*CH_2CH_2–	32.76
f	–CH_2*CH_2CO–	34.46
g	CH_3*CH_2CH_2–	23.47
h	–*CH_2CH_2CO–	25.60
i	—CH=*$CHCH_2CH_2$—	130.35
y	=*$CHCH_2$*CH=	128.73
z	–CH_2CH_2*CO–	172.43
TG-$C_{1,3}$	glycerol *CH_2	62.59
TG-C_2	glycerol *CH	69.74
shoulder on h	—CH=CH*CH_2CH=CH—	26.32

[a] Letter designations for resonances are as given in Figure 1c. *C indicates the specifically assigned type of carbon. After the spectrum shown in Figure 1c was measured, [3-^{13}C]alanine was added; chemical shifts were measured relative to alanine C-3 as an internal reference. Other resonances in Figure 1 are A at 40.4 ppm (unassigned) and B at 54.8 ppm [choline $(CH_3)_3N$–]. Assignments are from Hamilton et al. (1974) and Sears (1975).

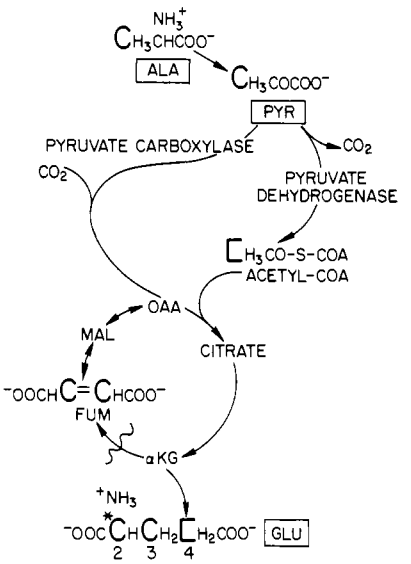

FIGURE 3: Simplified model pathway. The original label at C-3 of alanine (boldface C) is followed through pyruvate carboxylase into the tricarboxylic acid cycle, where in the symmetrical molecule fumarate (FUM) the label is found with equal probability at *either* of the two middle carbons (boldface C's). The two middle carbons of oxalacetate (OAA) label glutamate C-2 and C-3; the asterisk follows the position of the original, unscrambled label through pyruvate carboxylase and into glutamate C-2. The original label at C-3 of alanine is also followed through pyruvate dehydrogenase into acetyl-CoA, which is labeled only at C-2 (boldface squared C). C-2 of acetyl-CoA is followed into citrate and α-ketoglutarate (αKG) and, hence, into glutamate C-4 (boldface squared C).

As indicated schematically in Figure 3, when the only exogenous substrate present in perfused liver is [3-^{13}C]alanine, which is converted to [3-^{13}C]pyruvate, the proportion of pyruvate entering the TCA cycle by decarboxylation to [2-^{13}C]acetyl-CoA relative to the proportion entering by carboxylation to [3-^{13}C]oxalacetate can be estimated from the ^{13}C enrichment at glutamate C-4 relative the enrichments at glutamate C-2 and C-3. Figure 2a shows the ^{13}C NMR spectrum of a liver from a fed normal control rat after 40–50-min perfusion under conditions of metabolic and isotopic steady state in the presence of 10 mM [3-^{13}C]alanine. Glu-

Table II: NMR Measurement of ^{13}C Distribution in Glutamate in Perfused Liver from Normal and Streptozotocin-Diabetic Rats[a]

donor rat	relative ^{13}C enrichment of glutamate		
	C-4	C-3	C-2
diabetic (7)	39 ± 3	30 ± 1	70 ± 1
fed normal (3)	85	29	71
24-h-fasted normal (3)	13	30	70

[a] The isotopic distributions are from the integrated intensities of the glutamate signals in spectra of perfused liver metabolizing [3-^{13}C]alanine (10 mM) as the only exogenous substrate under steady-state conditions. Insulin (7 nM) was present in two of the perfusions of diabetic livers. The relative distributions were corrected for NOE and T_1 effects as described in the text. Results are given as the average of the number of perfused liver experiments given within parentheses. For each liver, four to five repetitive spectra also gave the same distribution to the error limits shown. The ^{13}C enrichments at glutamate C-1 and C-5 are given in the text.

tamate is strongly labeled at C-2, C-3, and, especially, C-4 in this liver. The ^{13}C enrichment at the directly labeled glutamate C-2 exceeds that at C-3. Label was detectable at glutamate C-2, C-3, and C-4 even 10-min postsubstrate and reached its steady-state distribution by 40–50-min postsubstrate Figure 2a). As described under Materials and Methods, the intensities measured under our conditions must be corrected for NOE and T_1 effects, which may affect different carbon atoms to varying extents; when these corrections are applied, the relative ^{13}C enrichments at glutamate C-4, C-3, and C-2 are 85, 29, and 71 in liver from fed control rats under our conditions (Table II). Livers from streptozotocin-diabetic rats were perfused in the presence of 10 mM [3-^{13}C]alanine under the same, steady-state conditions; representative ^{13}C NMR spectra acquired under these conditions have been reported (Cohen, 1987a). In diabetic liver the average relative ^{13}C enrichments at glutamate C-4, C-3, and C-2 were 39, 30, and 70. Under these same conditions the relative ^{13}C enrichments at glutamate C-3 and C-2 in perfused liver from 24-h-fasted control rats were also 30 and 70; however, the enrichment at C-4 was considerably less (Table II).

From the ^{13}C enrichments measured at glutamate C-4, C-3, and C-2 (Table II), we estimate that in liver from fed normal control rats the proportion of pyruvate entering the TCA cycle by the pyruvate dehydrogenase route relative to the pyruvate carboxylase route was 1:(1.2 ± 0.1); in liver from 24-h-fasted normal rats this ratio was 1:(7.7 ± 2); in liver from streptozotocin-diabetic rats the ratio was 1:(2.6 ± 0.3). Thus, the flux into the TCA cycle through the pyruvate carboxylase route relative to the flux into the TCA cycle through the pyruvate dehydrogenase route is estimated to be about 6.4-fold greater in liver from fasted control rats than in liver from fed controls. However, the flux through the pyruvate carboxylase route relative to that through the pyruvate dehydrogenase route is estimated to be only 2.2-fold greater in liver from the chronically diabetic rats than in liver from fed normal control rats. In diabetic liver, the relative proportion of pyruvate channeled into the TCA cycle through the two pathways was not altered by in vitro incubation with insulin (n = 2) (Table II).

[3-^{13}C]Alanine was selected as the substrate of choice for this ^{13}C NMR assay of the relative proportion of pyruvate entering the TCA cycle via the two competing routes because its use results in glutamate being principally labeled at carbons C-2, C-3, and C-4, all of which give rise to resonances that can be monitored with good sensitivity under our conditions in time-resolved spectra of perfused liver. The ^{13}C enrichments of glutamate C-1 and C-5 were also monitored since substantial labeling at these sites would affect any analysis of the competing pathways. Because of their longer T_1, the resonances of glutamate C-1 and C-5 are relatively more saturated under the acquisition conditions used for perfused liver. Therefore, to provide the most sensitive monitor, the distribution of label at these sites was measured in ^{13}C NMR spectra of perchloric acid extracts of the livers listed in Table II. Livers were freeze-clamped at the end of the perfusion period, and perchloric acid extracts were prepared (Materials and Methods). Because livers were perfused with [3-^{13}C]-alanine under steady-state conditions, these results are thought to be representative. Extracts of the livers represented in Table II showed no detectable ^{13}C label at glutamate C-5. Label at glutamate C-5 under these conditions would arise from the recycling of pyruvate with randomized label in the phosphoenolpyruvate cycle. As measured in the perchloric acid extracts, ^{13}C enrichment at glutamate C-1, which arises from activity of the TCA cycle, ranged from 1 to 7% of the total enrichment at glutamate C-1, C-2, and C-3 for the several livers listed in Table II. These measurements indicate that although no correction for enrichment at C-5 was required, neglect of the ^{13}C enrichment at glutamate C-1 resulted in an underestimation of the proportion of pyruvate that entered the TCA cycle by the pyruvate carboxylase route relative to the pyruvate dehydrogenase route of 7% or less, which is within the error limits indicated above for this ratio.

The proportion of pyruvate entering the TCA cycle as acetyl-CoA was greatest in liver from fed control rats by the ^{13}C NMR determination developed here. Because the contribution of acetyl-CoA to the extramitochondrial process of fatty acid synthesis is known to be maximal in liver of fed normal rats, livers from fed controls were perfused under our standard steady-state conditions, and the incorporation of ^{13}C label in fatty acids was followed. To demonstrate the applicability of ^{13}C NMR to the study of lipogenesis in perfused rat liver, labeled substrates that are converted to either [1-^{13}C]acetyl-CoA or [2-^{13}C]acetyl-CoA were used: (a) [2-^{13}C]pyruvate enters the TCA cycle via the pyruvate dehydrogenase route as [1-^{13}C]acetyl-CoA; (b) [3-^{13}C]alanine is converted to [2-^{13}C]acetyl-CoA via the activity of pyruvate dehydrogenase. In addition, the oxidation of [2-^{13}C]ethanol produces [2-^{13}C]acetate, which is also activated to [2-^{13}C]-acetyl-CoA in the liver cell by the cytosolic and mitochondrial acetyl-CoA synthetases (Goldberg & Brunengraber, 1980). In the de novo synthesis pathway, [2-^{13}C]acetyl-CoA is incorporated into fatty acids according to schema I, whereas

$$-OOC^{*}CH_2CH_2(\underbrace{^{*}CH_2CH_2}_{c,d})_{n/2}{}^{*}CH_2CH_2{}^{*}CH_3$$

z f h c,d e g a

I

[1-^{13}C]acetyl-CoA is incorporated into fatty acids according to schema II, where the lettering of carbons a–z is consistent

$$-OO^{*}CCH_2{}^{*}CH_2\underbrace{(CH_2{}^{*}CH_2)}_{c,d}{}_{n/2}CH_2{}^{*}CH_2CH_3$$

z f h c,d e g a

II

with the assignments in Table I and Figures 1, 2, 4, and 5. Note that here c,d refers to resonances c and d; no distinction between repeating methylene carbons is intended.

The spectra shown in Figure 2 provide an example of the operation of schema I. Although at 40–50 min after the initial addition of [3-^{13}C]alanine an intense resonance for glutamate C-4 is seen (Figure 2a), no ^{13}C enrichment in any fatty acyl chain carbon was measurable. However, by 40–50 min after the coadministration of [2-^{13}C]ethanol (Figure 2b), strong

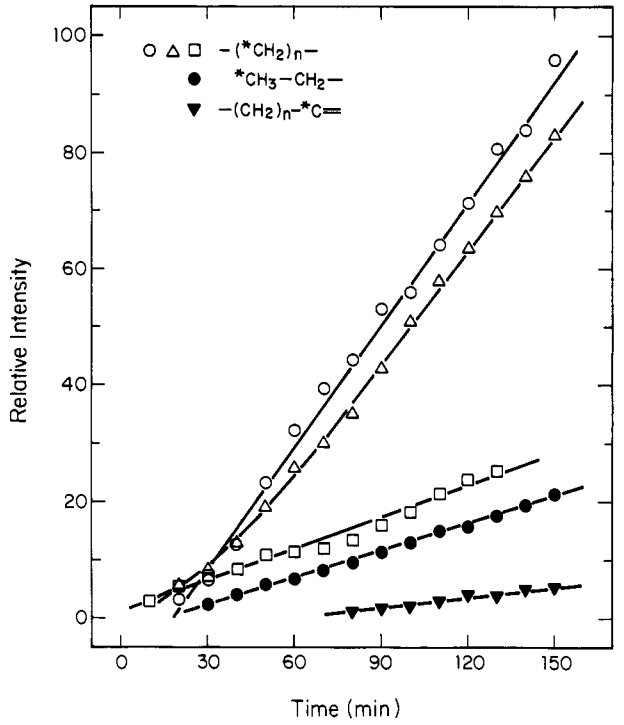

FIGURE 4: Time course of ^{13}C enrichment in fatty acyl carbons in perfused liver from fed normal control rats. Normalized signal intensities are from ^{13}C NMR spectra processed as described in Figure 2, in the absolute intensity mode. Livers were perfused under conditions of metabolic and isotopic steady state. Enrichment was measured at $-(*CH_2)_n-$ (peak d) for livers perfused with 10 mM [3-^{13}C]alanine + 7.3 mM [2-^{13}C]ethanol (n = 2) (△), with 9.1 mM [2-^{13}C]pyruvate, 5.5 mM NH_4Cl, and 7.3 mM ethanol (n = 2) (□), or with 9.1 mM [2-^{13}C]pyruvate, 5.5 mM NH_4Cl, and 7.3 mM [2-^{13}C]ethanol (n = 2) (○). ^{13}C enrichments at $*CH_3CH_2-$ (●) (peak a) and at $-(CH_2)_n*C=$ (▼) (peak i) are each given for the average of four liver perfusions, two with the [3-^{13}C]alanine + [2-^{13}C]ethanol substrate and two with the [2-^{13}C]pyruvate, NH_4Cl, and [2-^{13}C]ethanol substrate. Symbol size, in general, covers the range of normalized intensity values. Data points are plotted at the time coinciding with the midpoint of the corresponding spectrum; t = 0 corresponds to the initial addition of ethanol (unlabeled or labeled).

signals were measured for fatty acyl chain carbons a and c,d. The resonances labeled a, c, and d continued to increase in intensity throughout the balance of the perfusion (Figure 2c), as did that labeled i (Figure 2c insert showing spectral region of 125–135 ppm). It is notable that the only olefinic carbon enriched to detectable levels by lipogenesis under these conditions was that assigned to monoenoic fatty acids (peak i at 130.4 ppm); this circumstance is to be contradistinguished from that prevailing for endogenous fatty acids in ^{13}C natural abundance spectra of rat liver (Figure 1a,b) in which peak y at 128.7 ppm, which arises only from polyenoic fatty acids, gives the more intense olefinic carbon signal. In accord with schema I, no ^{13}C enrichment at the carbonyl carbon, z, was observed here (not shown). In Figure 2, the resonance assigned to carbon e is seen as a shoulder on the broad resonance arising from glutamine C-4 and GSH γ-glutamyl C-4. However, resonances arising from glutamate C-3 and glutamine C-3 interfer with peak b, and that from glutamate C-4 interfers with carbon f.

Representative spectra from this liver perfusion are presented in Figure 2; because spectra were accumulated continually, the time course of change in intensity of the various resonances is obtained. Figure 4 shows the increase in ^{13}C enrichment in the carbons of fatty acyl chains during this liver perfusion as a function of time of perfusion after the initial addition of [2-^{13}C]ethanol (t = 0); no enrichment in fatty acid

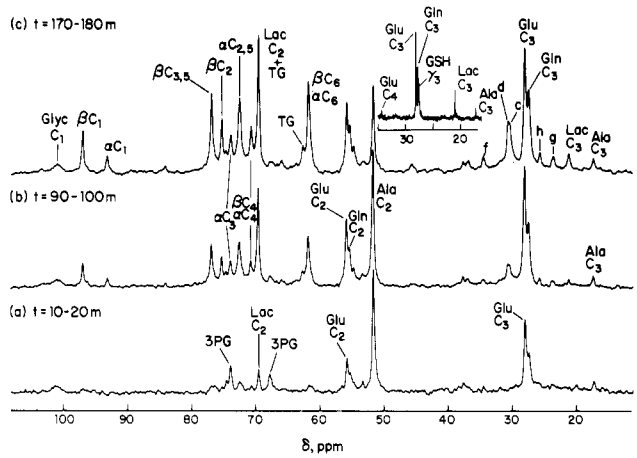

FIGURE 5: ^{13}C NMR spectra of perfused liver from a fed normal rat. The region between 10 and 110 ppm is shown. Spectra are part of a time sequence; spectrum a was measured 10–20 min after the addition of 9.1 mM [2-^{13}C]pyruvate and 5.5, mM NH_4Cl. Spectrum b was accumulated during the period 90–100 min after the addition of [2-^{13}C]pyruvate + NH_4Cl and 50–60 min after the addition of 7.3 mM unlabeled ethanol. Spectrum c was measured 170–180 min after the initial addition of [2-^{13}C]pyruvate + NH_4Cl and 140–150 min after initial addition of ethanol. Other conditions are as given for Figure 2. Abbreviations are as given in Figure 2, with the following additions: Glyc C_1, C-1 of glycosyl units in glycogen; peaks g, h, c, and d, assigned in Table I; peak f, discussed in the text. The insert shows the region from 16 to 35 ppm of the ^{13}C NMR spectrum of the perchloric acid extract of this liver, which was freeze-clamped shortly after spectrum c was measured. The pH of this extract was 8.44; the spectrum of the extract was measured under the conditions given for the extract in Figure 2.

carbons was detected prior to the addition of ethanol. As indicated in Figure 4, the ^{13}C enrichments at the repeating methylene carbons, peak d (△), at the terminal methyl carbon, peak a (●), and at the unsaturated carbon, peak i (▼), all increased monotonically with time of perfusion in the presence of [2-^{13}C]ethanol. (Note that the results for two liver preparations perfused with the substrate, [3-^{13}C]alanine plus [2-^{13}C]ethanol, which gave almost identical enrichments at carbons d, a, and i, are represented by the symbols △, ●, and ▼.) However, the rate of increase of ^{13}C enrichment at the repeating methylene carbons (peak d) was much greater than that at carbon a; increase of ^{13}C enrichment at the unsaturated carbon (peak i) proceeded at the slowest rate observed.

The spectra shown in Figure 5 demonstrate the operation of schema II. Here the labeled substrate, [2-^{13}C]pyruvate, is converted to [1-^{13}C]acetyl-CoA. Flow of ^{13}C label was followed from [2-^{13}C]pyruvate into alanine C-2 and C-3, glutamate and glutamine C-2, C-3, and C-5 (at 182.2 and 178.8 ppm, respectively, not shown), lactate C-2, 3-phosphoglycerate, and glycogen just 10 min after the addition of substrate (Figure 5a). However, no ^{13}C enrichment was observed in fatty acids until *unlabeled* ethanol was added at 40 min after the initial addition of [2-^{13}C]pyruvate. This circumstance is consistent with an intense requirement for reducing equivalents during fatty acid biosynthesis under our conditions, as discussed below; however, it is emphasized that [1-^{13}C]acetyl-CoA can only be derived from the [2-^{13}C]pyruvate substrate. By 90–100 min after the initial administration of [2-^{13}C]pyruvate and 50–60 min after the coaddition of unlabeled ethanol, signals for the fatty acyl chain carbons g, h, and c,d were seen (Figure 5b), as was the signal for the carbonyl carbon z (at 172.5 ppm, not shown). The resonances assigned to fatty acyl carbons g, h, c,d, and z increased monotonically throughout the balance of the perfusion period (Figure 5c) under these steady-state conditions. Note the

Table III: Relative ^{13}C Enrichments at Carbons in ^{13}C-Labeled Fatty Acids Synthesized by Perfused Livers from Fed Normal Rats[a]

relative peak areas	conditions		
	schema I	schema II	mixed schema I and II
z/g		1:(1 ± 0.05)	
z/a			1:(4 ± 0.06)
i/a	(0.06 ± 0.02):1		(0.06 ± 0.02):1
(c + d)/a	(5.0 ± 0.2):1		
(c + d)/(a + z)			(5.0 ± 0.2):1
(c + d)/h (or g)		(6.0 ± 0.2):1	

[a] In spectra of perfused liver, integrated areas of the peaks, labeled as in Table I, were corrected for T_1 and NOE effects as described in the text. Schema I, schema II, and mixed schema I and II conditions are given in the text and in Figure 4. Results are the average of $n = 2$ for each set of conditions.

absence of signal for the terminal methyl carbon a in Figure 5 in agreement with schema II, whereas carbons g, c,d, h, and z are labeled in schema II. No ^{13}C enrichment at an unsaturated carbon was observed here, presumably because of the lower level of enrichment in fatty acyl carbons. Again, the elimination of ^{13}C natural abundance background resonances for peaks A, y, i, and a in Figure 5a–c and peaks d and c in Figure 5a indicates the thoroughness of the procedure used to subtract out the natural abundance background spectrum of the liver. The time course for increase in ^{13}C intensity at peak d (□) for this perfused liver is plotted in Figure 4. (Although ^{13}C enrichment at the triacylglycerol backbone was also observed at 62.59 and 69.74 ppm in Figures 2 and 5, this label does not distinguish true biosynthesis from simple turnover of the pool.)

From observations of fatty acid biosynthesis under the conditions used for the perfused liver preparation represented in Figure 2, it seemed probable that the ^{13}C-labeled fatty acid synthesized by the liver preparation of Figure 5 represented only a fraction of this liver's total fatty acid production because the unlabeled ethanol present provided a source of unlabeled acetyl-CoA. Therefore, livers from fed control rats were perfused under the same steady-state conditions except that, 50 min after the initial addition of 9.1 mM [2-^{13}C]pyruvate + 5.5 mM NH_4Cl, 7.3 mM [2-^{13}C]ethanol was administered. The time courses of ^{13}C enrichment at several fatty acyl carbons under these conditions, which represent a mixture of schema I and schema II, are given in Figure 4. The rates of increase of ^{13}C enrichment at the terminal methyl group, carbon a (●), and at the unsaturated carbon i (▼) coincide with those observed for pure schema I conditions, whereas the rate of increase of ^{13}C enrichment at the repeating methylene carbon as measured at peak d (○) was slightly greater than that observed for pure schema I conditions.

No corrections for T_1 or NOE effects were made in the data shown in Figure 4. However, the T_1 and NOE measurements reported by Canioni et al. (1983) for the natural abundance of ^{13}C in fatty acyl chains in isolated rat liver at 90.5 MHz, together with natural abundance ^{13}C NMR spectra of neutral lipids in liver under our exact conditions (Figure 1c), provide the information needed for making such corrections. Observed integrated peak areas were corrected for T_1 and NOE effects in this way, and the several useful relationships given in Table III were obtained.

No resonances assignable to fatty acyl carbons (Table I) have been detectable in liver from either streptozotocin-diabetic rats or 24-h-fasted normal control rats under these same perfusion conditions (Cohen, 1987a). Only in liver from fed control rats, or, in certain instances, control rats fasted for 12 h or less, is biosynthesis of fatty acids observed.

The biosynthesis of ^{13}C-labeled glucose in liver from fed rats is demonstrated in Figures 2 and 5. Glucose concentrations in aliquots of perfusate taken at regular intervals throughout these perfusions were measured chemically as described previously (Cohen, 1987a). In liver from fed rats, the rates of glucose production measured in this way also contain contributions from the breakdown of endogenous glycogen; this total rate of glucose production was 28.0 ± 0.7 μmol (g of liver wet weight)$^{-1}$ h^{-1} for the six livers represented by the data in Figure 4.

Because the natural abundance distribution of ^{13}C is 1.1%, extraction of liver lipids into organic solvents, which is the usual procedure in $^{3}H/^{14}C$ isotopic studies, is not useful in ^{13}C NMR studies of the biosynthesis of fatty acids from ^{13}C-labeled precursors. That is, the large mass (Juggi & Prathap, 1979) of endogenous lipids that would also be extracted in this way from cellular membranes and neutral lipid droplets would give rise to resonances that would interfer with those associated with fatty acids produced from ^{13}C-labeled substrates via the de novo synthesis pathway. Therefore, an approach previously used by Doyle et al. (1981) was adapted for this study; this approach relies on the insolubility of fatty acids in perchloric acid. The inserts of Figures 2 (left-most insert) and 5 show the 15–40 ppm region of ^{13}C NMR spectra of the perchloric acid extracts of the respective livers, which were freeze-clamped shortly after the spectra shown in Figures 2c and 5c, respectively, were recorded. These perchloric acid extracts aided in the identification of the numerous acid-soluble metabolites present. Beyond this utility, absence of any resonances attributable to fatty acyl carbons in these perchloric acid extracts is consistent with their assignments in the corresponding spectra of liver. Thus, the peaks labeled a, c, d, and e in Figure 2c, which were assigned to fatty acyl carbons, clearly are not detectable in the left-most insert to Figure 2. Unfortunately, the regions labeled 8 and 5 in this insert overlap the chemical shifts of fatty acyl peaks f and b, respectively. The insert to Figure 5 clearly indicates that the metabolites responsible for the peaks labeled d, c, h, and g in Figure 5c were not extractable into perchloric acid, which is consistent with the assignment of these peaks to their respective fatty acyl carbons in schema II. The peak denoted as f in Figure 5c is at the chemical shift of both glutamate C-4 and fatty acyl carbon f, which is *not* labeled in schema II; however, the insert of Figure 5 shows that the metabolite giving rise to this peak was acid-soluble, which is consistent with its assignment to glutamate C-4. The introduction of a weak label at glutamate C-4 under these conditions has been described previously (Cohen, 1987b).

Discussion

The mitochondrial enzyme pyruvate carboxylase is possibly the rate-controlling step for gluconeogenesis from substrates that enter the pathway prior to the triose phosphate level and is implicated in hormonal control of gluconeogenesis from such precursors (Kraus-Friedmann, 1984). Only pyruvate entering the TCA cycle via pyruvate carboxylase as oxalacetate produces a net increase in mass of cycle intermediates, which is an absolute requirement for their being used in gluconeogenesis. Pyruvate entering via pyruvate dehydrogenase as acetyl-CoA is used in the cycle for energy production only. Because pyruvate dehydrogenase competes with pyruvate carboxylase for entry of pyruvate into the TCA cycle, the regulation of pyruvate dehydrogenase is also pertinent to the control of gluconeogenesis. In this study, the ^{13}C enrichments in the individual carbons of glutamate as measured in ^{13}C NMR spectra of perfused rat liver metabolizing [3-^{13}C]alanine

were used to estimate the relative proportion of pyruvate entering the TCA cycle by these two competing routes. In liver from fed control rats, the fluxes through these two routes were approximately equal by this ^{13}C NMR determination; however, in liver from either streptozotocin-diabetic or 24-h-fasted control rats, relatively more pyruvate entered the TCA cycle via the pyruvate carboxylase route. These observations generally correlate with the higher rates of gluconeogenesis measured in liver from diabetic or fasted control rats (Cohen, 1987a) and are consistent with our present observations of the biosynthesis of fatty acids in liver from fed rats but not from either diabetic or 24-h-fasted rats. In liver from diabetic or fasted control rats, [3-^{13}C]pyruvate, derived from [3-^{13}C]-alanine (Figure 3), entered the TCA cycle primarily as oxalacetate and thus strongly labeled glutamate C-2 and C-3 (Table II); the weak labeling measured at glutamate C-4, which is derived from acetyl-CoA, is consistent with the well-known decreased rate of lipogenesis and increased use of fatty acids in a major energy source that obtains for liver in vivo in fasted rats and in experimental models of type 1 diabetes (Lehninger, 1975). An increase in acetyl-CoA resulting from the oxidation of endogenous fatty acids is capable of decreasing the flux of ^{13}C label from [3-^{13}C]alanine to acetyl-CoA in three ways: inhibition of the pyruvate dehydrogenase complex (Reed, 1981); activation of pyruvate carboxylase (Utter & Scrutton, 1969); dilution of label by increasing pool size. Previous ^{13}C NMR measurements did not support the presence of significant endogenous acetyl-CoA in our isolated perfused liver preparation from fasted donor rats (Cohen, 1983), suggesting that simple dilution of label may not be a major factor in vitro.

This determination of the relative proportion of pyruvate entering the TCA cycle by the competing pyruvate dehydrogenase and pyruvate carboxylase routes is the ^{13}C NMR analogue of the pioneering in vivo ^{14}C isotopic methods of Freedman and Graff (1958) and Koeppe et al. (1959). These investigators carried out the demanding and time-consuming isolation and complete degradation of glutamate obtained from rat liver 1 or 3 h after the administration in vivo of either [2-^{14}C]alanine or [2-^{14}C]pyruvate; relative radioactivity was then measured for the individual glutamate carbon atoms. Agreement is excellent between the present ^{13}C NMR measurements and the ^{14}C method of Freedman and Graff (1958), who extracted glutamate from liver 1 h after the administration of [2-^{14}C]alanine in vivo. (The distributions at C-2/C-3 and at C-4/C-5 are, of course, reversed from those reported here because of their use of alanine labeled at C-2.) The agreement at C-1, C-2, C-3, and C-4 (our C-5) is almost exact for fasted rats. However, the ^{14}C enrichment at C-5 (our C-4) was about one-third of the corresponding ^{13}C enrichment measured in our isolated perfused liver preparations, which may reflect both dilution of label by a larger endogenous acetyl-CoA pool extant in liver in vivo and greater inhibition of pyruvate dehydrogenase because of the longer (40-h) period of fasting used by Freedman and Graff. Using [2-^{14}C]pyruvate and a 3-h incubation period in vivo, Koeppe et al. (1959) measured more randomization at glutamate C-1, C-2, and C-3 than found in this study or by Freedman and Graff (1958). As summarized by Katz (1985), however, Koeppe et al. (1959) determined that 8% of the glutamate ^{14}C activity was on C-5 in rats starved for 2 days, compared with 45% for fed control rats and 34% for a rat alloxan-diabetic 6 weeks; the corresponding glutamate activities measured here by ^{13}C NMR (Table II) are 12, 46, and 28%, respectively, which are in reasonable agreement.

The activity of pyruvate dehydrogenase is controlled by several intramitochondrial effectors, and thus, artifactual changes in the enzyme's activity during in vitro assays cannot be excluded (Ball & McLean, 1983); consequently, there is some interest in comparing this ^{13}C NMR determination of the competition for entry of pyruvate into the TCA cycle with in vitro assays of the corresponding enzymic activities. By ^{13}C NMR, the flux into the TCA cycle through the pyruvate carboxylase route relative to the pyruvate dehydrogenase route was estimated to be 6.4-fold greater in liver from fasted donor rats than in liver from fed normal control rats. Measurements reported by Caterson et al. (1982) indicate that pyruvate dehydrogenase activity is 2.5 times greater in liver from fed control rats than in liver from 48-h-fasted controls, whereas pyruvate carboxylase has been shown to be 2.5 times more active in liver from fasted control rats as compared with fed rats (Solling et al., 1973). An extrapolation from these in vitro assays suggests that the activity of pyruvate carboxylase relative to the activity of pyruvate dehydrogenase is 6.3 times greater in the fasted state compared to the fed state, in excellent agreement with the ^{13}C NMR value. By our ^{13}C NMR method, flux through pyruvate carboxylase relative to pyruvate dehydrogenase is 2.2 times greater in diabetic liver than in liver from fed normal control rats. Unfortunately, results from in vitro enzymic assays corresponding to our exact conditions of chronic diabetes are not available, and estimates based on various assays in which liver from alloxan-diabetic or streptozotocin-diabetic rats only 12-days posttreatment were used (Ball & McLean, 1983; Weinberg & Utter, 1980) give ratios at least 70% higher than the present ^{13}C NMR result.

The degree of randomization measured here (Table II) for glutamate C-2 and C-3 is consistent with the composite rate of mitochondrial malate dehydrogenase and fumarase exchange being 1.5 times the net rate of the TCA cycle in perfused liver under the present conditions, which is close to the value of 1.3 obtained in a previous study of liver perfused with similar substrates (Cohen, 1983).

The liver occupies the pivotal position in lipid metabolism, with the activities of the lipogenic enzymes of rat liver cytosol decreasing during a fast and increasing when fasted rats are refed (Van Golde & Van den Bergh, 1977). In this study, the application of ^{13}C NMR to the study of lipogenesis was demonstrated in perfused liver from fed normal control rats. The sensitivity of the method permitted serial observations with 10-min time resolution. Livers were perfused under conditions of metabolic and isotopic steady state with specifically labeled substrates that are converted to either [2-^{13}C]acetyl-CoA or [1-^{13}C]acetyl-CoA, which in the de novo synthesis pathway label alternate carbons in fatty acids according to either schema I or schema II, respectively. Time-sequential spectra of these livers (Figures 2, 4, and 5) showed increasing ^{13}C enrichment at fatty acyl carbon atoms labeled in a pattern characteristic of the appropriate schema. In addition to observation of specific resonances that distinguish schema I from schema II, resonances for the repeating methylene carbons that are common to both schemata were also measured in the time-resolved spectra. Several inferences can be drawn from these NMR measurements as summarized by the relationships given in Table III:

(1) It is possible to distinguish the contributions of chain elongation from those of the de novo synthesis pathway. For schema II conditions, that is, perfusion with [2-^{13}C]pyruvate + unlabeled ethanol, the ratio of ^{13}C enrichment at carbon z to that at carbon g was 1:1 (±0.05). Because incorporation of ^{13}C label into the carbonyl carbon, z, occurs by both de novo

and chain elongation pathways, whereas incorporation of label at carbon g, $-*CH_2CH_3$, in the terminal acetyl unit occurs only by the de novo synthesis pathway, it follows directly that the relative contribution of chain elongation of endogenous fatty acids with labeled acetyl-CoA units was minor.

(2) Average chain length for the ^{13}C-labeled fatty acids produced was estimated from the ratio of ^{13}C enrichment at $-(*CH_2)_n-$ to the enrichment at a carbon atom such as either the terminal $-*CH_3$ or $-*CH_2CH_3$, which gives rise to a ^{13}C NMR resonance that is not obscured by interferring signals from other labeled metabolites. For either schema I or mixed schema I and II conditions, the average ratio for the ^{13}C enrichment at the repeating methylene carbons, peaks c + d, to that at carbon a (or carbons a + z for the mixed conditions) was (5.0 ± 0.2):1. Because only one carbon of each acetyl unit is labeled, an average chain length of (2 × 5.0) + 6 = 16.0 ± 0.4 per molecule of fatty acid is inferred. For pure schema II conditions, the ratio of ^{13}C enrichment at peaks c + d to that at either carbon h or carbon g was (6.0 ± 0.2):1. Thus, an average chain length of 18.0 ± 0.4 per molecule of fatty acid is inferred in this instance. The principal product of the fatty acid synthase complex is palmitic acid (Van Golde & Van den Bergh, 1977; Wakil et al., 1983); this circumstance, taken with the estimate given in (1) above, is consistent with the product of the de novo synthesis pathway serving as substrate for chain elongation by an average of one acetyl unit under schema II conditions.

(3) From the time course for ^{13}C enrichment at the olefinic fatty acyl carbon atom, i, the proportion of the product of the de novo synthesis pathway that served as precursor for monoenoic acid was estimated. For either schema I or the mixed schema I and II conditions, the ratio of ^{13}C enrichment at carbon i to that at carbon a was 0.06 ± 0.02. Hence, about 6% of the product of the de novo synthesis pathway served as precursor for monoenoic acid.

(4) The rate of biosynthesis of ^{13}C-labeled fatty acid was obtained. This rate can be estimated from the average fatty acyl chain length and from the area of the resonances c + d of the repeating methylene carbons relative to the area of a reference compound of known concentration and ^{13}C enrichment, such as [3-^{13}C]alanine. For either schema I or mixed schema I and II conditions, the maximum rate of fatty acid synthesis observed here is estimated to be about 80 ± 10 μmol of acetyl units (g of dry weight liver)$^{-1}$ h^{-1}. This rate of synthesis is about half the rate measured by Brunengraber et al. (1974) by $^3H/^{14}C$ methods for livers perfused with 7 mM ethanol and 25 mM glucose; however, the donor rats used in this radioisotope study had been maintained on a diet known to induce fatty acid biosynthesis.

(5) For mixed schema I and II conditions, that is, perfusion with [2-^{13}C]pyruvate and [2-^{13}C]ethanol, the ratio of ^{13}C enrichment at carbon z to that at carbon a was 1:4 (±0.06). Therefore, about one-fifth of the cytosolic acetyl-CoA pool available for fatty acid synthesis was derived from [2-^{13}C]-pyruvate, while about $^4/_5$ of the pool was traceable to [2-^{13}C]ethanol.

Lipogenesis from ^{13}C-labeled acetyl-CoA was observed under our conditions only after coaddition of either labeled or unlabeled ethanol. As shown by the labeling of glutamate C-4 and C-5 (Figure 3, Table II), in perfused liver from fed control rats, about half of the entry of [^{13}C]pyruvate into the TCA cycle occurred via conversion to [^{13}C]acetyl-CoA. Thus, the requirement of the coaddition of ethanol implies that additional reducing equivalents, supplemental to those provided by the phosphogluconate pathway, were required for fatty acid

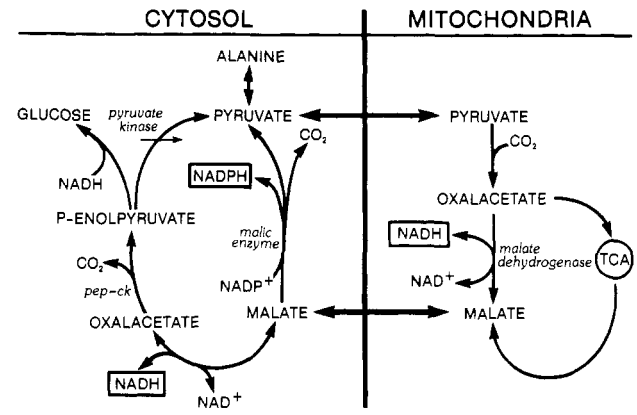

FIGURE 6: Simplified model pathway for transhydrogenation of NADH (from oxidation of ethanol, not shown) to cytosolic NADPH by coordination of the activities of malate dehydrogenase and the malic enzyme. *pep-ck* denotes phosphoenolpyruvate carboxykinase.

biosynthesis to occur in the presence of the oxidized substrates pyruvate and alanine. The synthesis of one molecule of palmitic acid, the major product of the de novo synthesis pathway, requires 14 molecules of NADPH; thus, it is not surprising that under our conditions fatty acid biosynthesis should require an additional system for generating NADPH in the cytosol. The oxidation of ethanol generates NADH in both the cytosol and the mitochondria. A probable mechanism for coupling NADH arising from the oxidation of ethanol to the generation of the NADPH needed for lipogenesis is provided by the coordination of malate dehydrogenase and malic enzyme activities (Young et al., 1964). The steps for this transhydrogenation of NADH to NADPH are shown schematically in Figure 6. In this well-established scheme (White et al., 1978), reducing equivalents are transferred from the mitochondria to the cytosol as malate, which is a common substrate of both malate dehydrogenase and the malic enzyme:

$$\text{oxalacetate}_m + \text{NADH}_m + \text{H}^+ \rightleftharpoons \text{malate}_m + \text{NAD}^+_m$$

$$\text{malate}_m \rightarrow \text{malate}_c$$

$$\text{malate}_c + \text{NADP}_c^+ \rightarrow \text{pyruvate}_c + \text{NADPH}_c + \text{CO}_2 + \text{H}^+$$

$$\text{sum: } \text{oxalacetate}_m + \text{NADH}_m + \text{NADP}_c^+ \rightarrow \text{pyruvate}_c + \text{CO}_2 + \text{NAD}^+_m + \text{NADPH}_c$$

where the subscripts m and c denote the mitochondrial and cytosolic compartments. As Figure 6 indicates, the carbons of alanine or pyruvate are also transferred to the cytosol as malate in the gluconeogenic pathway. The activity of phosphoenolpyruvate carboxykinase (PEP-CK) is minimal in liver from fed rats (Shrago et al., 1963), while the malic enzyme activity is decreased by fasting (Young et al., 1964); thus, both the low activity of PEP-CK and the elevated level of cytosolic NADH (from the oxidation of ethanol) tend further to favor increased flux through the malic enzyme and, hence, the production of NADPH (Figure 6). Other possible coupling mechanisms appear to be of less importance (Young et al., 1964). Thus, while ethanol is a source of acetyl-CoA, its critical role in promoting fatty acid synthesis in perfused liver under our conditions is considered to be the provision of NADH for the generation of NADPH by the coupling of malate dehydrogenase to the malic enzyme.

Although radioactivity methods have been used to infer pathways for the biosynthesis of lipids from $^3H/^{14}C$ ratios measured after incorporation of [^3H,^{14}C]acetate into fatty

acids (Goldberg & Brunengraber, 1980) and from decarboxylation experiments after incorporation of [1-^{14}C]acetate into fatty acids (Goodridge, 1973), the measurement of activities at several individual carbon atoms in fatty acyl chains by a ^{14}C isotopic analogue of the present ^{13}C NMR approach would almost certainly be too time consuming to be feasible. This circumstance renders the specificity of ^{13}C NMR in application to the study of lipogenesis in perfused rat liver particularly attractive. On the other hand, the 1.1% natural abundance distribution of ^{13}C in endogenous fatty acids in liver membranes and neutral lipid droplets precludes the extraction of the ^{13}C-labeled product of lipogenesis for the separation and measurement of the individual fatty acid components, as is possible with ^{14}C isotopic methods. In this initial ^{13}C NMR study of lipogenesis, the preparation of perchloric acid extracts of livers freeze-clamped at the termination of the perfusion period was considered to be an indispensable step in the identification of the various labeled metabolites. However, in future studies use of ^{14}C/^{13}C doubly labeled substrates, together with extraction of lipids into organic solvents at the end of the perfusion period, would permit acquisition of the complementary information afforded by the two techniques. As this investigation and its companion papers (Cohen, 1987a,b) may suggest, ^{13}C NMR spectroscopy provides a versatile way of examining metabolism in intact functioning liver, including the kinetics of lipogenesis and gluconeogenesis and the effects of hormonal treatment or fasting on the phosphoenolpyruvate cycle and on fluxes into the TCA cycle, in a manner that is complementary to existing ^{14}C methods and assays of enzymic activities.

ACKNOWLEDGMENTS

I thank MaryLou James for technical assistance and Stacianne Fischbach for typing the manuscript.

Registry No. Acetyl-CoA, 72-89-9; pyruvate dehydrogenase, 9014-20-4; pyruvate carboxylase, 9014-19-1; pyruvate, 127-17-3; glutamate, 56-86-0; alanine, 56-41-7; ethanol, 64-17-5.

REFERENCES

Ball, M. R., & McLean, P. (1983) *Enzymes (3rd Ed.) 29*, 15–20.

Block, R. E. (1982) *Biochem. Biophys. Res. Commun. 108*, 940–947.

Brunengraber, H., Boutry, M., Lowenstein, L., & Lowenstein, J. M. (1974) in *Alcohol and Aldehyde Metabolizing Systems* (Thurman, R. G., Yonetani, T., Williamson, J. R., & Chance, B., Eds.) pp 329–337, Academic, New York.

Canioni, P., Alger, J. R., & Shulman, R. G. (1983) *Biochemistry 22*, 4974–4980.

Caterson, I. D., Fuller, S. J., & Randle, P. J. (1982) *Biochem. J. 208*, 53–60.

Cohen, S. M. (1983) *J. Biol. Chem. 258*, 14294–14308.

Cohen, S. M. (1987a) *Biochemistry* (first paper of three in this issue).

Cohen, S. M. (1987b) *Biochemistry* (second paper of three in this issue).

Cohen, S. M., Shulman, R. G., & McLaughlin, A. C. (1979) *Proc. Natl. Acad. Sci. U.S.A. 76*, 4808–4812.

Cohen, S. M., Glynn, P., & Shulman, R. G. (1981) *Proc. Natl. Acad. Sci. U.S.A. 78*, 60–64.

Cross, T. A., Pahl, C., Oberhansli, R., Aue, W. P., Keller, U., & Seelig, J. (1984) *Biochemistry 23*, 6398–6402.

Doyle, D. D., Chalovich, J. M., & Bárány, M. (1981) *FEBS Lett. 131*, 147–150.

Freedman, A. D., & Graff, S. (1958) *J. Biol. Chem. 233*, 292–295.

Goldberg, R. P., & Brunengraber, H. (1980) in *Alcohol and Aldehyde Metabolizing Systems* (Thurman, R. G., Ed.) Vol. 4, pp 413–418, Plenum, New York.

Goodridge, A. G. (1973) *J. Biol. Chem. 248*, 1924–1931.

Hamilton, J. A., Talkowski, C., Childers, R. F., Allerhand, A., & Cordes, E. H. (1974) *J. Biol. Chem. 249*, 4872–4878.

Juggi, J. S., & Prathap, K. (1979) *Cytobios 24*, 117–134.

Katz, J. (1985) *Am. J. Physiol. 248*, R391–R399.

Koeppe, R. E., Mourkides, G. A., & Hill, R. J. (1959) *J. Biol. Chem. 234*, 2219–2222.

Kraus-Friedmann, N. (1984) *Physiol. Rev. 64*, 170–259.

Krebs, H. A. (1957) *Endeavor 16*, 125–132.

Lehninger, A. L. (1975) *Biochemistry*, pp 846–847, Worth, New York.

Menahan, L. A. (1983) *Metabolism 32*, 172–178.

Neurohr, K. J., Grollin, G., Neurohr, J. M., Rothman, D. L., & Shulman, R. G. (1984) *Biochemistry 23*, 5029–5035.

Oxley, S. T., Proteous, R., Brindle, K. M., Boyd, J., & Campbell, I. D. (1984) *Biochim. Biophys. Acta 805*, 19–24.

Reed, L. J. (1981) *Curr. Top. Cell. Regul. 18*, 95–106.

Reo, N. V., Siegfried, B. A., & Ackerman, J. J. H. (1984) *J. Biol. Chem. 259*, 13664–13667.

Sears, B. (1975) *J. Membr. Biol. 20*, 59–73.

Shrago, E., Lardy, H. A., Nordlie, R. C., & Foster, D. O. (1963) *J. Biol. Chem. 238*, 3188–3192.

Solling, H. D., Kleineke, J., Willms, B., Janson, G., & Kuhn, A. (1973) *Eur. J. Biochem. 37*, 233–243.

Stevens, A. N., Iles, R. A., Morris, P. G., & Griffiths, J. R. (1982) *FEBS Lett. 150*, 489–493.

Utter, M. F., & Scrutton, M. C. (1969) *Curr. Top. Cell. Regul. 1*, 253–296.

Van Golde, L. M. G., & Van der Bergh, S. G. (1977) in *Lipid Metabolism in Mammals* (Snyder, F., Ed.) Vol. 1, pp 35–39, Plenum, New York.

Wakil, S. J., Stoops, J. K., & Joshi, V. C. (1983) *Annu. Rev. Biochem. 52*, 537–579.

Weinberg, M. B., & Utter, M. F., (1980) *Biochem. J. 188*, 601–608.

White, A., Handler, P., Smith, E. L., Hill, R. L., & Lehman, R. I. (1978) *Principles of Biochemistry*, pp 372–383, McGraw-Hill, New York.

Williams, E., Hamilton, J. A., Jain, M. K., Allerhand, A., & Cordes, E. H. (1973) *Science (Washington, D.C.) 181*, 869–871.

Young, J. W., Shrago, E., & Lardy, H. A. (1964) *Biochemistry 3*, 1687–1682.